Letter

Microscopic origin of the spin-induced linear and quadratic magnetoelectric effects

Maocai Pi, Xifan Xu, Mingquan He, and Yisheng Chai*
Center of Quantum Materials and Devices, Chongqing University, Chongqing 401331, China
and Low Temperature Physics Laboratory, College of Physics, Chongqing University, Chongqing 401331, China

(Received 27 September 2021; accepted 22 December 2021; published 18 January 2022)

Understanding of the intimate cross coupling between electric and magnetic degrees of freedom in solids usually requires sophisticated models and time-consuming calculation methods. Instead of macroscopic symmetry analysis, we present a simple but general approach to explore the microscopic mechanism of magnetoelectric (ME) effects in magnetic ordered materials based on local spin and lattice symmetry analysis. Our method is successfully applied to Cr_2O_3 and orthorhombic RMnO$_3$ with linear and quadratic ME effects, respectively. We revealed all the possible microscopic origins of every nonzero ME coefficient that cannot be easily fulfilled by other theoretical methods. Moreover, the contribution from each mechanism can be located down to specific spins or spin pairs. Our theoretical approach is capable of providing a detailed guide on exploring rich spin-induced magnetoelectrics with strong ME effects.

DOI: 10.1103/PhysRevB.105.L020407

Crystals with long-range magnetic orders can lead to emergent phenomena as cross coupling between electric and magnetic degrees of freedom, e.g., magnetoelectric (ME) effect or spin-induced polarization (type-II multiferroics). Based on the global symmetry of magnetic ordering, a macroscopic polarization (P) can be induced if the space inversion symmetry is broken. A linear ME effect is allowed if both time reversal and space inversion symmetries are broken. So far, the microscopic origins of spin-induced polarization have been mainly studied by first-principles calculation, and are attributed to three main mechanisms, including two-spin mechanisms [exchange-striction, inverse Dzyaloshinskii-Moriya (DM) mechanism] and single-spin mechanism (p-d hybridization mechanism) [1–3]. However, the local symmetric information in type-II multiferroics has not been fully utilized. Nevertheless, a lattice site-symmetry approach was introduced to find the microscopic mechanisms in high crystal symmetric systems [4–7]. For example, the spin-induced polarization in $LaMn_3Cr_4O$ with antiferromagnetic ordering in cubic lattice is resolved to be an antisymmetric exchange-striction mechanism [8].

The ME effects can be linear (LME) or quadratic (QME), i.e., the electric polarization P (magnetization M) responses linearly or quadratically to the application of magnetic field H (electric field E). The corresponding coupling coefficients can be defined as $\alpha = P/H(\mu_0 M/E)$ or $\beta = P/H^2(\mu_0 M/E^2)$, respectively. As a physical principle to realize electronic devices, the ME effect has attracted considerable interest [9,10]. Despite remarkable progress in composite ME materials and related devices [11], the ME devices made by spin-induced ME materials are still very rare due to their weak coupling strength [12]. The most typical LME material Cr_2O_3 in antiferromagnetic (AFM) order has a maximum α value of 7 ps/m [13], while the orthorhombic RMnO$_3$ (R is rare earth ions) with E-type AFM ground states shows a quadratic response of P to H [14,15] with a small β value. Besides the Cr_2O_3, the microscopic mechanisms of linear or quadratic ME effects are less explored in other single-phase materials due to the lack of theoretical treatments. To find more magnetic systems with giant ME effects, a universal theoretical approach is highly desired to reveal the microscopic origins of LME and QME effects or even higher order effects.

In this Letter, we developed a general theoretical approach to understand the microscopic origins of LME and QME effects simultaneously. Based on the site symmetries of lattice and spin together, we elucidate the role of each mechanism and each spin pair in the LME effects in Cr_2O_3 which was omitted previously. In the orthorhombic RMnO$_3$, we reveal that their QME coupling coefficients in the E-type AFM state have two dominating nonzero components governed only by the exchange striction mechanism. Our comprehensive approach could also be applicable to other single phase ME materials and to the ME effects above the second order.

From atomic scale, the microscopic origin of electric dipoles, whether they are induced from the type-II multiferroics or from the magnetic ordered magnetoelectrics under H, would not have much difference. To reveal such similarity qualitatively, one can always describe the local electric dipole $\boldsymbol{p} = \boldsymbol{p}_{12} + \boldsymbol{p}_{11} + \boldsymbol{p}_{22}$ from a spin pair S_1 and S_2 irrespective of multiferroics or magnetoelectrics. In general, the coupling between S_1 and S_2 produces the local electric dipole $\boldsymbol{p}_{12}$, while the local dipoles $\boldsymbol{p}_{11}$ and $\boldsymbol{p}_{22}$ are produced by spins S_1 and S_2, respectively, with their surrounding ligand atoms. Both $\boldsymbol{p}_{ii}$ and $\boldsymbol{p}_{ij}$ $(i, j = 1, 2)$ can be expressed as functions with the two variables S_1 and S_2 under the second order Taylor expansion in the Einstein convention:

$$\boldsymbol{p}_{ii}^{\gamma} = P_{ii}^{\alpha\beta\gamma} S_i^{\alpha} S_i^{\beta}, \boldsymbol{p}_{ij}^{\gamma} = P_{ij}^{\alpha\beta\gamma} S_i^{\alpha} S_j^{\beta}, \tag{1}$$

where superscripts α, β, and γ represent the Cartesian coordinates x, y, z. $P_{ii}^{\alpha\beta\gamma}$ and $P_{ij}^{\alpha\beta\gamma}$ are the local third-rank

*Corresponding author: yschai@cqu.edu.cn

magnetoelectric tensors corresponding to single spin with ligand atoms and spin pair, respectively. Only even-order terms in the coefficients of Taylor expansion are reserved because of time reversal symmetry. The macroscopic $P = (P^x, P^y, P^z)$ is

$$P^\gamma = \sum_{i,j} P_{ij}^{\alpha\beta\gamma} S_i^\alpha S_j^\beta, \tag{2}$$

where i, j run over all spins and adjacent spin pairs. This local ME tensor analysis has been successfully applied to explain the microscopic origin of P in multiferroics in the absence of magnetic field [4–8] [see the Supplemental Material (SM) for more details [16]]. When a small H is applied, the change of spin configuration in either type-II multiferroics or magnetoelectrics would induce a small change in polarization, $\delta P = P(H) - P(0\,\mathrm{T})$, which is indeed the ME effect.

The spin vector $S_i(H)$ at atom i can be expanded as, in the Einstein convention:

$$S_i(H) = S_i(0) + \frac{\partial S_i^\alpha}{\partial H^l} H^l + \frac{\partial^2 S_i^\alpha}{2\partial H^l \partial H^m} H^l H^m + \cdots, \left(\frac{\partial S_i^\alpha}{\partial H^l} = A_i^{\alpha l}, \ \frac{\partial^2 S_i^\alpha}{2\partial H^l \partial H^m} = B_i^{\alpha lm} \right), \tag{3}$$

where α, l, and m run over the Cartesian coordinates x, y, z. $A_i^{\alpha l}$ and $B_i^{\alpha lm}$ are linear and quadratic local spin susceptibility tensors under a small H, respectively. Based on the symmetry analysis, $A_i^{\alpha l}$ is invariant under both space inversion and time reversal symmetry, and has the same transformation properties as the macroscopic susceptibility tensor. On the other hand, $B_i^{\alpha lm}$ is invariant with space inversion symmetry but opposite with time reversal symmetry, which has the same transformation properties as the macroscopic piezomagnetic coefficient tensor.

The above spin variations lower the symmetry of the magnetic materials, which causes the variation of δP by putting Eq. (3) into Eq. (2):

$$\begin{aligned} P^\gamma(H) &= \sum_{i,j} P_{ij}^{\alpha\beta\gamma} \left[\left(S_i^\alpha + A_i^{\alpha l} H^l + B_i^{\alpha lm} H^l H^m + \cdots \right) \right. \\ &\quad \left. \times \left(S_j^\beta + A_j^{\beta l} H^l + B_j^{\beta lm} H^l H^m + \cdots \right) \right] \\ &= \sum_{i,j} P_{ij}^{\alpha\beta\gamma} S_i^\alpha S_j^\beta + \sum_{i,j} P_{ij}^{\alpha\beta\gamma} \left(S_j^\beta A_i^{\alpha l} + S_i^\alpha A_j^{\beta l} \right) H^l \\ &\quad + \sum_{i,j} P_{ij}^{\alpha\beta\gamma} \left(S_i^\alpha B_j^{\beta lm} + S_j^\beta B_i^{\alpha lm} + A_i^{\alpha l} A_j^{\beta m} \right) H^l H^m \\ &\quad + \cdots . \end{aligned} \tag{4}$$

The first term is polarization without H, which is zero for pure ME systems like Cr_2O_3 but is finite for multiferroics like o-RMnO$_3$ with E-type AFM. The second and third terms describe the δP induced by LME and QME effects, respectively. Then, the mathematical expressions of related ME tensor can be derived from Eq. (4) accordingly. All the terms and related information to calculate each macroscopic property are summarized in Table I. Furthermore, we are able to infer the microscopic mechanisms of ME effects from the nonzero components of $P_{ii}^{\alpha\beta\gamma}$ and $P_{ij}^{\alpha\beta\gamma}$ in δP (see SM for details [16]). For the converse ME effects with the magnetization response to the external electric field, the method proposed in this work cannot be applied directly.

TABLE I. Required local information to calculate macroscopic physical properties.

	$P_{ii}^{\alpha\beta\gamma}$ or $P_{ij}^{\alpha\beta\gamma}$	S_i	$A_i^{\alpha l}$	$B_i^{\alpha lm}$
Spin-induced ferroelectricity	√	√		
LME effect	√	√	√	
QME effect	√	√	√	√

We first apply this approach to the most well-known LME material, Cr_2O_3. The AFM order appears below $T_N = 307$ K, showing in Fig. 1(a). Its magnetic point group is $-\mathbf{3}'m'$ with the symmetry operations $m' \perp x$ and $-\mathbf{3}' \parallel z$. According to Neumann's principle, the nonzero LME coefficients α^{ij} are $\alpha^{xx} = \alpha^{yy} = \alpha_\perp$ and $\alpha^{zz} = \alpha_{||}$ whose variations strongly rely on the magnetic susceptibilities. The temperature dependent $\alpha_\perp$ decreases smoothly upon cooling, whereas $\alpha_{||}$ shows a peak below T_N which drops quickly and becomes negative as approaching 0 K which comes from Van Vleck paramagnetism [13,17]. The positive peak feature below T_N is considered to be mainly due to the exchange striction mechanism [18]. The agreement between other existing theories and experiments is very good in the case of $\alpha_\perp$ but fails in that of $\alpha_{||}$ [19]. These calculations, however, cannot tell all the possible microscopic origins and detailed locations responsible for the observed LME effects in this system [18].

To resolve the problems mentioned above, we evaluate the LME components $\alpha_\perp$ and $\alpha_{||}$ from our theory. The starting AFM at $H = 0$ would be: $S_1 = S_4 = -S_2 = -S_3 = (0, 0, S^z)$, where the magnetic moments of Cr spins S_1, S_2, S_3, and S_4 form a magnetic period. Under external H, the local linear spin susceptibility tensor $A_i^{\alpha l}$ of spin at atom i (i = 1–4) has only three nonzero components after excluding the Van Vleck paramagnetism, i.e., $A_i^{xx} = A_i^{yy} = \chi_{i\perp}$ and $A_i^{zz} = \chi_{i\|}$. Such a simplifying process is based on the Wyckoff symmetry $\mathbf{3}_z$ of the Cr atoms. Based on the crystal symmetries, we found that all the S_i have identical local spin susceptibility tensor $\chi_{i\perp} = \chi_\perp$ and $\chi_{i_{||}} = \chi_{||}$.

Then, we can determine the single-spin tensor $P_{ii}^{\alpha\beta\gamma}$ by Cr moment at atom i (i = 1–4). Based on the global $\mathbf{3}_z$ symmetry in the crystal lattice, the symmetric matrix form of $P_{ii}^{\alpha\beta\gamma}$ is simplified by Neumann's principle that $\mathbf{3}_z P_{ii}^{\alpha\beta\gamma} = P_{ii}^{\alpha\beta\gamma}$ as follows [4]:

$$P_{ii}^{\alpha\beta\gamma} = \begin{pmatrix} P_{ii}^{xxx}, P_{ii}^{xxy}, P_{ii}^{xxz} & P_{ii}^{xxy}, -P_{ii}^{xxx}, 0 & P_{ii}^{xzx}, P_{ii}^{xzy}, 0 \\ P_{ii}^{xxy}, -P_{ii}^{xxx}, 0 & -P_{ii}^{xxx}, -P_{ii}^{xxy}, P_{ii}^{xxz} & -P_{ii}^{xzy}, P_{ii}^{xzx}, 0 \\ P_{ii}^{xzx}, P_{ii}^{xzy}, 0 & -P_{ii}^{xzy}, P_{ii}^{xzx}, 0 & 0, 0, P_{ii}^{zzz} \end{pmatrix} \tag{5}$$

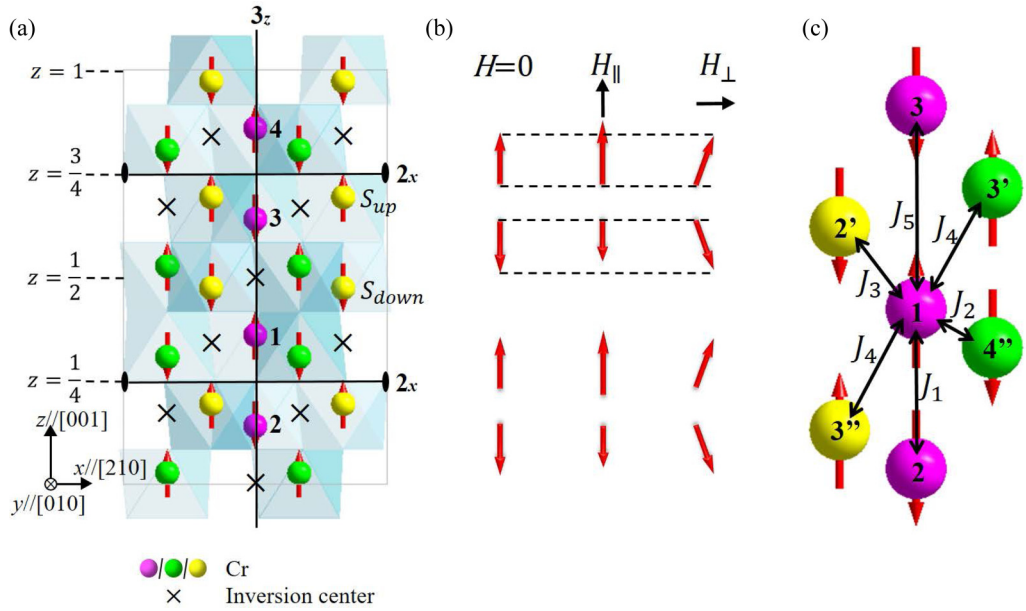

FIG. 1. (a) The crystal structure and AFM structure of Cr_2O_3. Space inversion centers and threefold axis along the z direction are indicated. (b) The schematic diagram of the spins variations on four purple Cr atoms under different magnetic fields applied, when H is applied along the spin direction, the parallel spins and antiparallel spins tend to elongate and shorten, respectively. When H is perpendicular to the spin direction, all spins deflect towards the magnetic field direction. (c) Spin pairs (J_1–J_5) between every Cr atom with its six nearest neighbors, of which J_2, J_4, and J_3 represent all three bonds connected by the threefold symmetry in the z direction.

As for the two-spin tensor $P_{ij}^{\alpha\beta\gamma}$ between adjacent atoms i and j, there are five different nearest exchange couplings J_1 to J_5 that contribute to the observed LME effects [20], as shown in Fig. 1(c), corresponding to the local two-spin tensors $P_{1,2}$, $P_{1,4''}$, $P_{1,2'}$, $P_{1,3'}$, and $P_{1,3}$ respectively. The related $P_{ij}^{\alpha\beta\gamma}$ are simplified by symmetry operations as well (see the SM for details [16]).

Finally, the polarization P at zero magnetic field $H = 0$, and δP that are induced by δH along the x and z directions of Cr_2O_3 are calculated by substituting all local ME tensors and the initial spin vectors S_i and $A_i^{\alpha l}$ into Eq. (4) (see the SM for details [16]). The first term of P under zero H is calculated to be exactly zero, consistent with the LME nature of Cr_2O_3. The second LME terms show finite response of polarization δP with $\alpha_\perp = \delta P^x/\delta H^x$ and $\alpha_{||} = \delta P^z/\delta H^z$:

$$\alpha_\perp \propto \left(2P_{11}^{xzx} - 2P_{12}^{xzx} + 2P_{13'}^{zxx} + 2P_{13'}^{xzx} + P_{12'}^{zxx} - P_{12'}^{xzx} + P_{14''}^{zxx} - P_{14''}^{xzx}\right)\chi_\perp S^z, \tag{6}$$

$$\alpha_\parallel \propto \left(P_{11}^{zzz} + P_{13'}^{zzz}\right)\chi_\parallel S^z, \tag{7}$$

where P_{11}^{zzz} and P_{11}^{xzx} come from a single-spin tensor, while the rest of the coefficients originate from the two-spin tensors. One can see that $\alpha_{||}$ and $\alpha_\perp$ are proportional to $\chi_{||}$ and $\chi_\perp$, respectively, which are fully consistent with previous theoretical studies and experimental observations. More importantly, both single-spin tensor and two-spin tensor contribute to $\alpha_{||}$ and $\alpha_\perp$, which was not anticipated in the previous studies [13,17–21] that neglect single-spin terms as $p_{ii}^x = P_{ii}^{xzx}\delta S_i^x S_i^z$ and $p_{ii}^z = 2P_{ii}^{zzz}\delta S_i^z S_i^z$. From the matrix form of p-d hybridization mechanism, both terms are allowed (see the SM for details [16]). In terms of two-spin tensors, $P_{13'}^{zzz}$ is allowed in the exchange striction mechanism, while $(P_{12'}^{zxx} - P_{12'}^{xzx})$, $(P_{14''}^{zxx} - P_{14''}^{xzx})$, and P_{12}^{xzx} are nonzero in the inverse DM mechanism. Note that the $P_{13'}^{zxx} + P_{13'}^{xzx}$ is exactly zero in both two-spin mechanisms (see the SM for details [16]), but is allowed in the antisymmetric exchange mechanism proposed by Xiang [8]. To conclude for Cr_2O_3, our approach suggests that $\alpha_\perp$ is originated from the p-d hybridization mechanism with single spin, and the inverse DM mechanism from J_1, J_2, and J_3, possibly with a small contribution from J_4 with other mechanisms. The $\alpha_{||}$, on the other hand, is mainly controlled by the p-d hybridization mechanism and the exchange mechanism from J_4. All the calculated results are summarized in Table II. Our findings are consistent with previous studies but provide much better details down to atomic scale [18,21].

We then apply this approach to the multiferroic material with possible QME effects, the manganites $R\mathrm{MnO_3}$ with orthorhombic crystal structure. o-$R\mathrm{MnO_3}$ has the $Pbnm$ space group, including symmetric operations of inversion symmetry $\{-1|\ 0,0,0\}$, twofold rotation along the z axis $\{2_{001}|1/2, 0, 1/2\}$, and twofold rotation along the y axis $\{2_{010}|0, 1/2, 0\}$, as shown in Fig. 2. The neutron diffraction study and pyroelectric measurements confirm that below 40 K, o-$R\mathrm{MnO_3}$ (R = Lu, Ho, Gd, Eu...) polycrystalline samples show ferroelectricity with E-type AFM ordering of Mn spins [14], as shown in Fig. 2(a). Theoretical predictions have indicated that E-type AFM can break the space inversion symmetry and bring out huge ferroelectric polarization in o-$R\mathrm{MnO_3}$ via the exchange striction mechanism [14,22] which is partially confirmed in experiments [14,15]. Dominating quadratic ME effects were clearly observed in both poly and single crystal o-$R\mathrm{MnO_3}$ in experiments [14,15]. However, the existence of ME effects in this system are not well

TABLE II. The calculated nonzero single or two-spin tensor components, LME coefficients, QME coefficients in Cr_2O_3 and RMnO$_3$, and the related microscopic mechanisms.

	Exchange Striction	Inverse DM interaction	p-d hybridization	Anisotropic symmetric exchange
Cr_2O_3	$P^{zzz}_{13'}:\alpha_{\parallel}, J_4$	$(P^{zxx}_{12'}-P^{xzx}_{12'}):\alpha_{\perp}, J_3$ $(P^{zxx}_{14''}-P^{xzx}_{14''}):\alpha_{\perp}, J_2$ $P^{xzx}_{12}:\alpha_{\perp}, J_1$	$P^{xzx}_{11}:\alpha_{\perp}$ $P^{zzz}_{11}:\alpha_{\parallel}$	$P^{zxx}_{13'}+P^{xzx}_{13'}:\alpha_{\perp}, J_4$
o-RMnO$_3$	$P^{xxz}_{12}:\beta^{zyy},\beta^{zzz}$	$(P^{xyy}_{12}-P^{yxy}_{12}):\beta^{yyz}$		$(P^{xzx}_{12}+P^{zxx}_{12}):\beta^{zyy}$ $(P^{xzy}_{12}+P^{zxy}_{12}):\beta^{yyz}$

explained either on magnetic symmetry or down to microscopic level.

We first consider whether the magnetic symmetry of E-type AFM allows the ME effects in o-RMnO$_3$. The magnetic point group of o-RMnO$_3$ with Mn E-type AFM ground state is ***mm*21′**, which is a polar group supporting ferroelectricity. Here, we do not consider the ordering of R ions. It belongs to the magnetic "grey group" with an independent time reversal operation, which is unable to generate any LME effect but QME effect, consistent with the experimental observations [14,15]. The expected QME tensor β^{ijk} can be written down in an abbreviated matrix form of [23]

$$\beta^{ijk}=\begin{pmatrix}0&0&0&0&Q_{15}&0\\0&0&0&Q_{24}&0&0\\Q_{31}&Q_{32}&Q_{33}&0&0&0\end{pmatrix}. \quad (8)$$

It is symmetrical with $\beta^{ijk}=\beta^{ikj}$ and we follow the convention: $Q_{31}=\beta^{zxx}$, $Q_{32}=\beta^{zyy}$, $Q_{33}=\beta^{zzz}$, $Q_{24}=\beta^{yyz}$, $Q_{15}=\beta^{xxz}$.

To calculate the components β^{ijk} from our theory, the starting AFM spin configuration at $H=0$ would be $S_{\rm up}=(S^x,0,0)$ and $S_{\rm down}=(-S^x,0,0)$. Under small external δH, the spin at atom i has local linear and quadratic spin susceptibility tensors $A_i^{\alpha l}$ and $B_i^{\alpha lm}$, respectively. No simplification can be made on those local susceptibility tensors. As for the single-spin tensor $P_{ii}^{\alpha\beta\gamma}$ for the Mn atom at site i, it will be exactly zero due to the on-site inversion symmetry. The measured polarization and QME in o-RMnO$_3$ are merely due to Mn-Mn interactions. All the spin pairs related to $P_{ij}^{\alpha\beta\gamma}$ in the magnetic unit cell can be deduced from symmetry operations (see the SM for details [16]).

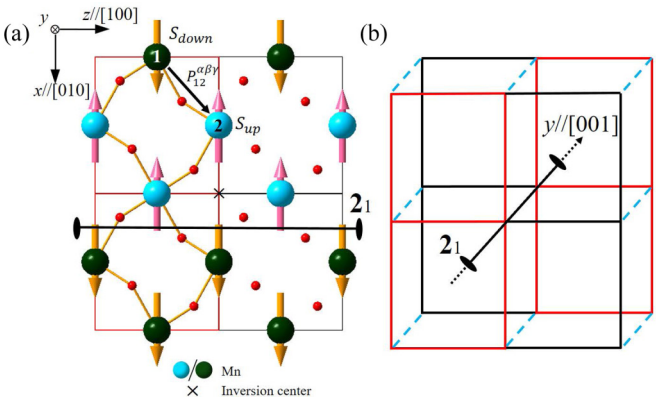

FIG. 2. (a) The location or spin configuration of Mn and oxygen atoms in xz plane in o-RMnO$_3$ lattice; (b) $\mathbf{2_1}$ symmetry operation between two atomic layers.

Similarly, following the procedure of Cr_2O_3, we can evaluate $P(H=0)$ and δP using Eq. (4) by inserting the two-spin tensors, the initial spin vectors $S_{\rm up}$ and $S_{\rm down}$, and $A_i^{\alpha l}$ and $B_i^{\alpha lm}$ (see the SM for details [16]). The first term in $P(H=0)$ reads out easily as $P\propto -8(S^x)^2(0,0,P_{12}^{xxz})$, with P_{12}^{xxz} originating from exchange striction between intralayer interactions, agreeing well with previous theoretical studies [14]. The second term in the LME of δP appears to be exactly zero, which is consistent with the magnetic point group analysis. Finally, finite QME coefficients emerge from the third terms:

$$\begin{aligned}\beta^{zii}&\propto -8S^x\left[2P_{12}^{xxz}B_1^{xii}+\left(P_{12}^{xyz}+P_{12}^{yxz}\right)B_1^{yii}+\left(P_{12}^{zxz}-P_{12}^{xzz}\right)B_1^{zii}\right],\\&\quad \text{where } i=x,y,\\ \beta^{jjz}&\propto 16S^x\left[\left(P_{12}^{xyj}-P_{12}^{yxj}\right)B_1^{yjz}-\left(P_{12}^{xzj}+P_{12}^{zxj}\right)B_1^{zxz}\right],\\&\quad \text{where } j=x,y,\\ \beta^{zzz}&\propto 16S^x\left[2P_{12}^{xxz}B_1^{xzz}+\left(P_{12}^{xyz}+P_{12}^{yxz}\right)B_1^{yzz}\right.\\&\quad \left.+\left(P_{12}^{zxz}-P_{12}^{xzz}\right)B_1^{zzz}\right], \quad (9)\end{aligned}$$

which is quite consistent with magnetic point group argument. Note that $A_i^{\alpha l}$ and interlayer interactions do not contribute to the QME in o-RMnO$_3$ directly. In terms of $B_1^{\alpha lm}$ for spin 1 with $(-S^x,0,0)$, we could assume that under small δH along the principle axis, the AFM spin configuration will change according to Fig. 1(b) by simply changing their magnitude or pure rotating in xz or xy planes. As a result, for $H\parallel x$, B_1^{xxx}, B_1^{yxx}, $B_1^{zxx}=0$, for $H\parallel y$ and z, B_1^{yxz}, B_1^{zyy}, and $B_1^{yzz}=0$ due to constraint of pure spin rotating, B_1^{yyy} and $B_1^{zzz}=0$ due to ideal linear $\chi_{\perp}$, while B_1^{yyz}, B_1^{zxz}, B_1^{xyy}, and B_1^{xzz} can be nonzero. It can be easily found that $B_1^{xyy}=(A_1^{yy})^2/2S^x$ and $B_1^{xzz}=(A_1^{zz})^2/2S^x$, respectively while B_1^{yyz} and B_1^{zxz} would be relatively much smaller. From above assumptions, β^{zxx} must be zero. In order to find out the dominating mechanisms responsible for the QME observed in experiments, we need to find out the possible mechanisms for each P_{ij}^{xxz} and the relative magnitude of $B_1^{\alpha lm}$ in AFM orders. In terms of two spin tensors, P_{12}^{xxz} is allowed in the exchange striction mechanism while $(P_{12}^{xyy}-P_{12}^{yxy})$ is nonzero in inverse DM mechanism. Note that the $(P_{12}^{xzx}+P_{12}^{zxx})$ and $(P_{12}^{xzy}+P_{12}^{zxy})$ are exactly zero in both mechanisms, but allowed in antisymmetric exchange mechanism proposed by Xiang [8]. In most cases, they are very small. Eventually, the dominating nonzero β^{ijk} would be $\beta^{zyy}\propto$

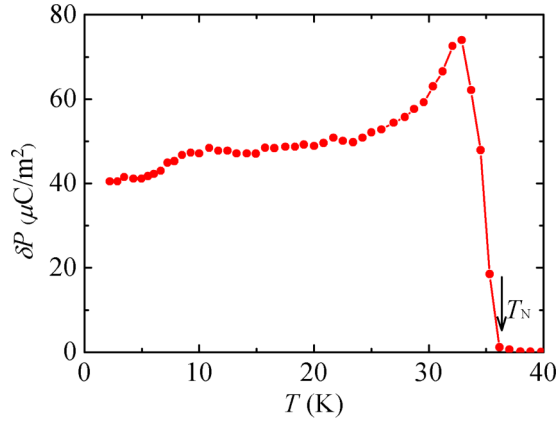

FIG. 3. The variation of polarization $\delta P = P(0\mathrm{T}) - P(14\mathrm{T})$ under 14 T in polycrystalline o-LuMnO3 [14].

$P_{12}^{xxz}(A_1^{yy})^2$, $\beta^{zzz} \propto P_{12}^{xxz}(A_1^{zz})^2$. $\beta^{zyy} \propto S^x(P_{12}^{xzx} + P_{12}^{zxx})B_1^{zxz}$ and $\beta^{yyz} \propto S^x[(P_{12}^{xyy} - P_{12}^{yxy})B_1^{yyz} - (P_{12}^{xzy} + P_{12}^{zxy})B_1^{zxz}]$ would be very small. All the calculated results are summarized in Table II.

We can compare our results with the experimental data. In the single crystal o-$TbMnO_3$ under pressure, it also has an E-type AFM ground state. The external $H \parallel z$ can induce a huge, quadratic change of P along z above Tb ordering temperature, indicating a nonzero β^{zzz}. In the polycrystalline o-$LuMnO_3$ [14], we find that the change of δP under 14 T is almost invariant below 20 K, as shown in Fig. 3, which is consistent with the almost constant $\chi_\perp$ in AFM orders. In conclusion, the QME of o-$RMnO_3$ mainly comes from the exchange striction mechanism, the same as that of its original spin-induced polarization and is proportional to the square of $\chi_\perp$.

In summary, we develop a general approach to explore the microscopic mechanisms of spin-induced ME effects in single phase multiferroics and magnetoelectrics. Our findings are consistent with experiments and previous studies with much better details down to atomic scale.

This work was supported by Natural Science Foundation of China Grants No. 11674384 and No. 11974065. This work has been supported by the Chongqing Research Program of Basic Research and Frontier Technology, China (Grant No. cstc2020jcyj-msxmX0263), Fundamental Research Funds for the Central Universities, China (Grants No. 2020CDJQY-A056, No. 2020CDJ-LHZZ-010, and No. 2020CDJQY-Z006), and Projects of President Foundation of Chongqing University, China (Grant No. 2019CDXZWL002).

M.C.P. and X.F.X. contributed equally in this work.

[1] Y. J. Choi, H. T. Yi, S. Lee, Q. Huang, V. Kiryukhin, and S.-W. Cheong, Phys. Rev. Lett. **100**, 047601 (2008).
[2] T. Kimura, Y. Seiko, H. Nakamura, T. Siegrist, and A. Ramirez, Nat. Mater. **7**, 291 (2008).
[3] H. Murakawa, Y. Onose, S. Miyahara, N. Furukawa, and Y. Tokura, Phys. Rev. Lett. **105**, 137202 (2010).
[4] Y. S. Chai, S. H. Chun, J. Z. Cong, and K. H. Kim, Phys. Rev. B **98**, 104416 (2018).
[5] H. J. Xiang, E. J. Kan, Y. Zhang, M.-H. Whangbo, and X. G. Gong, Phys. Rev. Lett. **107**, 157202 (2011).
[6] T. A. Kaplan and S. D. Mahanti, Phys. Rev. B **83**, 174432 (2011).
[7] S. Miyahara and N. Furukawa, Phys. Rev. B **93**, 014445 (2016).
[8] J. S. Feng and H. J. Xiang, Phys. Rev. B **93**, 174416 (2016).
[9] D. S. Shang, Y. S. Chai, Z. X. Cao, J. Lu, and Y. Sun, Chin. Phys. B **24**, 068402 (2015).
[10] S. H. Chun, Y. S. Chai, B. G. Jeon, H. J. Kim, Y. S. Oh, I. Kim, H. Kim, B. J. Jeon, S. Y. Haam, J. Y. Park, S. H. Lee, J. H. Chung, J. H. Park, and K. H. Kim, Phys. Rev. Lett. **108**, 177201 (2012).
[11] G. Srinivasan, Annu. Rev. Mater. Res. **40**, 153 (2010).
[12] S. Dong, J. M. Liu, S. W. Cheong, and Z. F. Ren, Adv. Phys. **64**, 519 (2015).
[13] V. J. Folen, G. T. Rado, and E. W. Stalder, Phys. Rev. Lett. **6**, 607 (1961).
[14] S. Ishiwata, Y. Kaneko, Y. Tokunaga, Y. Taguchi, T.-h. Arima, and Y. Tokura, Phys. Rev. B **81**, 100411(R) (2010).
[15] T. Aoyama, K. Yamauchi, A. Iyama, S. Picozzi, K. Shimizu, and T. Kimura, Nat. Commun. **5**, 4927 (2014).
[16] See Supplemental Material at http://link.aps.org/supplemental/10.1103/PhysRevB.105.L020407 for the details of symmetry analysis, and tensor and polarization calculations.
[17] D. N. Astrov, Sov. Phys. JETP **13**, 729 (1961).
[18] M. Mostovoy, A. Scaramucci, N. A. Spaldin, and K. T. Delaney, Phys. Rev. Lett. **105**, 087202 (2010).
[19] G. T. Rado and V. J. Folen, J. Appl. Phys. **33**, 1126 (1962).
[20] E. J. Samuelsen, M. T. Hutchings, and G. Shirane, Physica **48**, 13 (1970).
[21] R. Hornreich and S. Shtrikman, Phys. Rev. **161**, 506 (1967).
[22] S. Picozzi, K. Yamauchi, B. Sanyal, I. A. Sergienko, and E. Dagotto, Phys. Rev. Lett. **99**, 227201 (2007).
[23] H. Grimmer, Ferroelectrics **161**, 181 (1993).